

# Integration of Contracted Renewable Energy and Spot Market Supply to Serve Flexible Loads<sup>★</sup>

Anthony Papavasiliou<sup>\*</sup> Shmuel S. Oren<sup>\*\*</sup>

<sup>\*</sup> *Department of Industrial Engineering and Operations Research,  
UC Berkeley (e-mail: tonypap@berkeley.edu).*

<sup>\*\*</sup> *Department of Industrial Engineering and Operations Research,  
UC Berkeley (e-mail: oren@ieor.berkeley.edu).*

---

**Abstract:** We present a contract for integrating renewable energy supply and electricity spot markets for serving deferrable electric loads in order to mitigate renewable energy intermittency. The contract which we describe results in a stochastic optimal control problem for minimizing the cost of serving flexible load. We solve the optimal control problem by using a recombinant lattice for modeling renewable power supply and electricity spot price uncertainty. We compare various control policies, and we analyze the sensitivity of our results with respect to various problem parameters.

*Keywords:* Renewable energy, demand response, dynamic programming, recombinant lattices, model-predictive control.

---

## 1. INTRODUCTION

The proliferation of renewable energy sources in the United States is taking place at an unprecedented pace. The federal government is coordinating these efforts, with state regulations further advancing renewable energy integration targets. The American Clean Energy and Security Act (2009) set a target of sourcing 20% of US electricity consumption from renewable energy by 2020 and also set various goals for limiting reliance on nonrenewable resources. In 2002, the state of California enacted the Participating Intermittent Resources Program, which facilitates the integration of renewable energy sources. The California Renewable Portfolio Standard requires 20% of energy supply in the state to be sourced from renewable sources by 2012.

In the California ISO renewable integration report, Loutan and Hawkins (2007) voiced concerns about the impacts of large scale renewable energy integration on the capacity requirements and ramping requirements of load following and regulation services. These increased reserve requirements represent a significant barrier for the large scale integration of renewable power. An alternative to the costly investment in backup generation capacity is to exploit the flexibility of electricity demand. In close analogy to the policy coordination that is taking place for renewable energy integration, demand-side management is also being coordinated both at the federal level and in individual states. The American Clean Energy and Security Act (2009) has allocated \$3.4 billion in order

to spawn the development and deployment of the necessary technology to enable active management of electricity demand. Anticipating the importance of demand-side flexibility, the California electricity market rules have been adapted in order to accommodate the participation of demand resources through the recent Market Redesign and Technology Upgrade of 2007. Two of the major state utilities, San Diego Gas and Electric and Pacific Gas and Electric, are deploying smart metering throughout their respective service areas.

The most efficient approach for exploiting demand-side flexibility would be to establish real-time pricing at the retail level, a possibility which is discussed by Borenstein et al. (2002). However, there is strong political opposition to this approach as it exposes retail consumers to the volatility of electricity prices. In an alternative approach, which is described by Hirst and Kirby (1999) and Kirby (2003), flexible loads can participate in the ancillary services market. An aggregator could bid on behalf of a population of loads for providing capacity services to the system operator and would coordinate load consumption either through prices or direct control. The technical feasibility of demand side aggregation for the provision of spinning reserve has been studied in practice by Eto (2007). However, it is necessary to define market products that correspond to the types of ancillary services that loads can actually offer, which raises the need for reform in existing electricity markets.

In this paper we analyze a direct contractual agreement between deferrable loads and renewable generators. In the proposed contract, loads request a certain quantity of energy within a deadline. An aggregator is then responsible for serving these requests within their deadlines by relying primarily on renewable resources and, to a limited extent,

---

<sup>★</sup> This research was funded by NSF Grant IIP 0969016, the US Department of Energy through a grant administered by the Consortium for Electric Reliability Technology Solutions (CERTS), the Siemens Corporation under the UC Berkeley CKI initiative and the Federal Energy Regulatory Commission.

on the real-time market. The proposed contract closely matches dynamic scheduling, as described in Hirst and Kirby (1997), whereby demand and supply resources from different control areas coordinate their schedules in order to produce zero net output to the remaining system. Dynamic scheduling is currently implemented in the Electric Reliability Council of Texas.

The specification of demand flexibility in terms of requests for a fixed amount of energy within a fixed time horizon is a natural description for a wide variety of flexible energy needs, such as EV charging, water pumping, and various residential consumptions. There is also a natural complementarity between coupling renewable resources with deferrable requests. Due to the fact that renewable power supply is more predictable over a certain time horizon than in any given moment in time, it is easier to fulfill requests that extend over a time window. In addition, the contract relieves the system operator from the obligation of procuring reserves for protecting against intermittent renewable supply since renewable resources appear "behind the meter". The significant capital savings that stem from avoided investment in backup reserves can be shared with deferrable loads in order to incent their flexible behavior. Although the coupled system may resort to the spot market to a limited extent, the coupling contract effectively transfers the risk of renewable power variability from the system operator to deferrable loads.

A disadvantage of the proposed approach is that the bilateral commitment between loads and renewable generators results in trading inefficiencies. Coupling also reduces the effect geographical smoothing in renewable energy supply. Moreover, the contract requires direct load control by the aggregator, which might be undesirable to consumers.

For coupling contracts to work, renewables must be exposed to some of the risk they impose on the system. This can be achieved by forcing renewable suppliers to bid in the day-ahead market with a penalty for deviation, by removing feed-in tariffs, or by exposing renewable suppliers to the risk of spilling excess wind.

The model is formulated in section 2. In section 3 we present simulation results.

## 2. MODEL

In this section we formulate the optimal control problem that a renewable power supplier faces under our proposed contract. The supplier has the task of serving a flexible consumer from a freely available renewable resource which is backed up by a spot market for electricity. Wind generation and the spot price of electricity are driven by two correlated mean-reverting Ornstein-Uhlenbeck processes. The aggregator procures energy from the spot market with the objective to minimize the cost of unserved energy and expenditures in the spot market. We solve the optimal control problem by using dynamic programming. In particular, we use recombining lattices for modeling the electricity prices and wind power supply, following the methodology which is outlined in Deng and Oren (2003) and Deng and Oren (2005).

### 2.1 Price and wind models

We consider 8 day types in our analysis, which represent weekdays and weekends for each season. We use the Weibull distribution for modeling wind power generation, and the lognormal distribution for modeling prices. Both processes are driven by an underlying first-order autoregressive process which obeys the following dynamic model:

$$\begin{aligned} n_{t+1}^s &= n_t^s + \kappa^s(\theta^s - n_t^s)\Delta t + \sigma^s\omega_1\sqrt{\Delta t} \\ n_{t+1}^\lambda &= n_t^\lambda + \kappa^\lambda(\theta^\lambda - n_t^\lambda)\Delta t + \rho\sigma^\lambda\omega_1\sqrt{\Delta t} + \\ &\quad \sqrt{(1-\rho^2)}\sigma^\lambda\omega_2\sqrt{\Delta t}, \end{aligned} \quad (1)$$

where  $n_t^s$  and  $n_t^\lambda$  are the noise terms of the wind and price models respectively,  $\omega_1$  and  $\omega_2$  are independent standard normal random variables,  $\Delta t$  is the time step,  $\theta^s$  and  $\theta^\lambda$  represent the average trends of the wind and price noise respectively, the variance terms  $\sigma^s$  and  $\sigma^\lambda$  capture the effect of random shocks,  $\kappa^s$  and  $\kappa^\lambda$  model the rate at which the processes return to their mean value and  $\rho$  is a correlation coefficient which couples the evolution of the two processes.

Wind power supply is strongly influenced by seasonal and diurnal effects. Most and Keles (2009) discuss the need to remove these deterministic effects from the data in order to obtain the residual process which can be used for calibrating the parameters of the mean-reverting process. The seasonal and diurnal patterns of wind generation are captured by  $\mu_t^s$ , the average value of hourly wind production for each day type. We assume that the ratio  $\frac{s_t}{\mu_t^s}$  follows the Weibull distribution with parameters  $k, \lambda$ . Following Eq. 1 of Torres et al. (1984), section 2.1 of Torres et al. (2005) and Eq. 2 of Morales et al. (2010) for transforming Weibull-distributed data to Gaussian data, as well as the nonparametric transformation that is used in Eqs. 8, 9 of Callaway (2010), we use the inverse transform sampling method to obtain wind power,  $s_t$ , as a function of the underlying noise,  $n_t^s$ , and the real-time price signal  $\lambda_t$  as a function of  $n_t^\lambda$ :

$$\begin{aligned} s_t &= \mu_t^s \lambda \exp(k^{-1} \log \log(1 - N(n_t^s))) \\ \lambda_t &= \mu_t^\lambda \exp(n_t^\lambda), \end{aligned} \quad (3)$$

where  $s_t$  is the value of wind generation,  $\lambda_t$  is the real time electricity price,  $\mu_t^s$  and  $\mu_t^\lambda$  are the average values of hourly wind production and hourly real-time electricity prices respectively, and  $N(\cdot)$  is the cumulative distribution function of the normal distribution.

### 2.2 Problem Formulation

The dynamic optimization problem has a three-dimensional state vector,  $x_t = (\lambda_t, s_t, r_t)$ , where  $\lambda_t$  is the spot price of electricity,  $s_t$  is the amount of wind which is freely available and  $r_t$  represents the remaining quantity of demand. The residual energy  $r_t$  evolves according to  $r_{t+1} = r_t - u_t\Delta t$ , where  $u_t$ , our control, is the amount of power supplied to the consumer in period  $t$ . We model the two-dimensional stochastic process  $(\lambda_t, s_t)$  with a trinomial recombining lattice model. In particular, the dynamics of the underlying process are assumed to obey the following:

$$n_{t+1}^{s,j} = \begin{cases} n_t^s + \sigma^s \sqrt{\frac{3}{2}} \sqrt{\Delta t}, & j = 1 \\ n_t^s, & j = 2 \\ n_t^s - \sigma^s \sqrt{\frac{3}{2}} \sqrt{\Delta t}, & j = 3 \end{cases} \quad (5)$$

$$n_{t+1}^{\lambda,j} = \begin{cases} n_t^\lambda + (\sqrt{3}\rho + \sqrt{1-\rho^2})\sigma^\lambda \sqrt{\frac{\Delta t}{2}}, & j = 1 \\ n_t^\lambda - \sigma^\lambda \sqrt{1-\rho^2} \frac{2}{\sqrt{2}} \sqrt{\Delta t}, & j = 2 \\ n_t^\lambda - (\sqrt{3}\rho - \sqrt{1-\rho^2})\sigma^\lambda \sqrt{\frac{\Delta t}{2}}, & j = 3. \end{cases}$$

Each state  $j$  is visited with a probability  $p^j(n_t^\lambda, n_t^s)$  which depends on the current state. The transition probabilities are defined in Deng and Oren (2005).

The use of a recombinant lattice is motivated by computational efficiency. Note from the dynamics of Eqs. 5 that a given point in the state space in period  $t + 1$  can be visited by various points in the state space in period  $t$ . In effect, it is shown in Deng and Oren (2003) that the size of the state space grows quadratically in the horizon of the problem, which is to be contrasted to an exponential growth in the size of the state space when a trinomial lattice does not recombine. As a result, we are able to control the growth of the state space, and this enables us to solve the optimal control problem using the dynamic programming algorithm. Deng and Oren (2003) also prove that the transition probabilities and state space can be constructed such that, as  $\Delta t$  converges to zero, the discrete process converges in distribution to the continuous time mean reverting Ornstein-Uhlenbeck process.

In order to calibrate the wind model parameters, we used the 2006 National Renewable Energy Laboratory (NREL) database for an integration level of 14,143 MW in California. The upper frame of Fig. 1 shows the sample cumulative distribution function of the trinomial wind generation model overlaid on the sample cumulative density function of the wind dataset. The lower frame of Fig. 1 shows the cumulative distribution function of the electricity price lattice model.

The objective of the optimal control problem is to minimize the following expected cost:

$$\min_{\phi_t(x_t)} \mathbb{E} \left[ \sum_{t=1}^N \lambda_t (\mu_t(x_t) - s_t)^+ \Delta t + \rho r_N \right], \quad (6)$$

where  $\phi_t(x)$  represents the rate at which the resource is supplied and  $N$  is the number of periods. The state vector has the following initial condition:  $r_1 = R$ , where  $R$  is the amount of energy demand to be satisfied. The control  $u_t$  cannot exceed an upper bound on the rate of supply,  $u_t \leq C_p$ . In the case where power is supplied to  $n$  electric vehicle batteries,  $C_p$  equals  $nC$ , where  $C$  is the nominal rating of an electric vehicle battery. We also limit the amount of energy that can be procured in the real-time electricity market at each period to  $C_m$  by introducing the constraint  $u_t - s_t \leq C_m$  in order to transfer the risk of wind power variability from the system operator to the aggregator. Since the coupled system may rely only up to  $C_m$  on system reserves, there is a possibility that residual demand may not be fully satisfied. Unsatisfied

Table 1. Locations and capacity of wind power

| County      | 14143 MW | Existing MW |
|-------------|----------|-------------|
| Tehachapi   | 6459     | 722         |
| Clark       | 1500     | -           |
| Solano      | 583.45   | 327         |
| San Geronio | 528      | 624         |
| San Diego   | 1527     | -           |
| Humboldt    | 218.2    | -           |
| Imperial    | 547.9    | -           |
| Altamont    | 14       | 954         |
| Monterey    | -        | 118         |
| Pacheco     | -        | 21          |

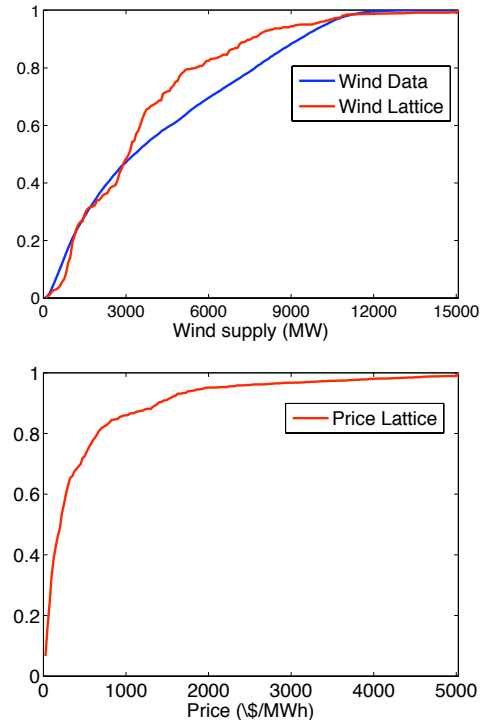


Fig. 1. Probability density function of wind output (top) and real time electricity prices (bottom) for deep wind integration case.

energy incurs a penalty  $\rho$ . Finally, we denote as  $K$  the nameplate capacity of renewable power resource.

### 3. RESULTS

#### 3.1 Data

As we mentioned in section 2.1, we have estimated parameters for eight day types, corresponding to weekdays and weekends of each season. The wind data used in this study is sourced from the NREL 2006 western wind database. The locations of the wind generation sites that are used for the study represent an integration target of 14,143 MW, based on the data presented in the CAISO report by Loutan and Hawkins (2007) and the 2010 California generation interconnection queue in CAISO (2010). There is a total of 2,648 MW of wind power currently connected in the California system. The locations of the wind sites are presented in table 1. Wind data was sampled from the NREL database according to the locations that are described in table 1.

We solve the problem for 24 hourly intervals. We consider 6 levels of charge for the control problem. The baseline level of wind integration is  $K = 14,143$  MW, corresponding to the 33% California renewable integration target, and the baseline capacity constraint of consumers is  $C_p = 15,000$  MW. We also impose a limit of  $C_m = 2,000$  MW in spot market participation. We have chosen  $C_m$  to be a small fraction of  $C_p$  in order to test our intuition that deferrable energy requests couple well with renewable power supply over an extended time horizon. If the coupled system were required to resort primarily to the real time market in order to perform adequately, then there is little reason to consider coupling contracts as a means of utilizing demand flexibility to absorb renewable supply fluctuations. The baseline level of total energy demand is  $R = 80,000$  MWh, which is 80 percent of the average daily wind output in the 33% wind integration target. The requests span over 24 hours. If we assume that a typical electric vehicle has a power rating of 3.6 kW and a mileage of 0.25 kWh per mile, the baseline demand model roughly represents the electricity demand of 4.167 million electric vehicles which travel 96 miles per vehicle per day. The cost of unserved energy in the baseline is  $\rho = 5,000$  \$/MWh. This value is selected as an estimate of the average cost of not serving flexible energy requests for vehicle charging.

### 3.2 Relative performance of policies

We now compare the performance of the dynamic programming policy, the clairvoyant policy which has advance knowledge of the outcome in each realization, a naive charging policy whereby consumers are served as fast as possible, and a model predictive control policy. The model predictive controller applies the optimal solution in step  $k$  to the optimal control problem that results if the stochastic processes were to follow their unperturbed dynamics for the remaining horizon.

The real-time market expenses of all policies are compared in table 2 for the baseline scenario. The second column represents the cost of the clairvoyant policy in bold type. The other columns present the relative performance of the other three policies with respect to the clairvoyant policy. The results are then averaged according to the frequency of each day type, and the relative real-time market costs of each policy are presented in both dollar figures as well as a percentage of the cost of the clairvoyant policy in the last two rows of the table. The overall performance of all policies, including the penalty of unserved energy, is compared in table 3. As in table 2, the results are presented relative to the clairvoyant policy. We observe that although model predictive control performs better than the naive policy in terms of real-time market expenditures, overall it performs worse than the naive policy due to the fact that it incurs high penalties for unserved energy.

### 3.3 Sensitivity on load capacity ( $C_p$ )

The sensitivity of the results on the capacity of the load are presented in Fig. 2. The first frame describes the relative real-time market expenses of the three policies. Beyond  $C_p = 10,000$  MW the system is not achieving any significant gains by further increasing load capacity, since it is relatively infrequent that wind generation exceeds

Table 2. Cost of procuring electricity from the real-time market (baseline scenario).

|             | Cost<br>(\$)<br><b>Clair</b> | $\Delta$ Cost<br>(\$)<br>Naive | $\Delta$ Cost<br>(\$)<br>MPC | $\Delta$ Cost<br>(\$)<br>Dyn Prog |
|-------------|------------------------------|--------------------------------|------------------------------|-----------------------------------|
| WinterWD    | <b>164,420</b>               | 1,325,680                      | 165,580                      | 241,640                           |
| SpringWD    | <b>85,289</b>                | 952,011                        | 111,611                      | 167,471                           |
| SummerWD    | <b>2,157,500</b>             | 976,100                        | 467,400                      | 321,900                           |
| FallWD      | <b>1,001,900</b>             | 1,348,500                      | 599,000                      | 462,000                           |
| WinterWE    | <b>169,250</b>               | 1,453,850                      | 177,570                      | 265,280                           |
| SpringWE    | <b>96,988</b>                | 1,102,712                      | 150,912                      | 177,532                           |
| SummerWE    | <b>1,770,200</b>             | 1,093,100                      | 455,700                      | 305,600                           |
| FallWE      | <b>1,132,200</b>             | 1,612,000                      | 693,500                      | 511,800                           |
| Total       | <b>835,086</b>               | 1,197,671                      | 345,474                      | 303,053                           |
| improv. (%) |                              | 143.4                          | 41.4                         | 36.3                              |

Table 3. Relative performance of policies (baseline scenario).

|             | Cost<br>(\$)<br><b>Clair</b> | $\Delta$ Cost<br>(\$)<br>Naive | $\Delta$ Cost<br>(\$)<br>MPC | $\Delta$ Cost<br>(\$)<br>Dyn Prog |
|-------------|------------------------------|--------------------------------|------------------------------|-----------------------------------|
| Market      | <b>835,086</b>               | 1,976,671                      | 345,474                      | 303,053                           |
| Unserved    | <b>436,161</b>               | 0                              | 1,433,482                    | 12,500                            |
| Total       | <b>1,271,247</b>             | 1,197,671                      | 1,778,956                    | 315,553                           |
| improv. (%) |                              | 94.21                          | 139.9                        | 24.8                              |

this level. The second frame presents the percentage of wind that is shed on average. The naive policy places an upper bound on the amount of wind shedding, while the clairvoyant policy places a lower bound since it relies on wind power as much as possible. The last frame presents the mix that is used for serving load for the case of the dynamic programming policy. As  $C_p$  increases, spot market procurements are replaced by freely available wind power supply. It is notable that unserved energy is negligible even for  $C_p = 5,000$  MW.

### 3.4 Sensitivity on wind power capacity ( $K$ )

In Fig. 3 we present the sensitivity analysis results for varying  $K$ . We note that there is a significant amount of wind shedding for high  $K$ , with the naive policy becoming highly inefficient due to the fact that it is not taking advantage of the excess supply of wind. We also note that there is a significant amount of unserved energy for the case of low  $K$ . The first frame shows that all policies incur almost the same cost at the real-time market, because it is almost always optimal to buy as much as possible from the real-time market.

### 3.5 Sensitivity analysis on spot market participation ( $C_m$ )

The sensitivity analysis on the degree of spot market participation is shown in Fig. 4. From the first frame we observe that despite the fact that  $C_m$  increases, the performance of the clairvoyant does not improve relative to the performance of the dynamic programming policy. As  $C_m$  increases, the naive policy becomes remarkably inefficient due to exposure in the spot market. In the second frame we note that as  $C_m$  increases the naive policy procures more power from the market and uses less wind. In the last frame we observe that for  $C_m = 1,000$  MW a notable amount of load is unserved, while as  $C_m$  increases wind is replaced by market procurements and unserved energy diminishes.

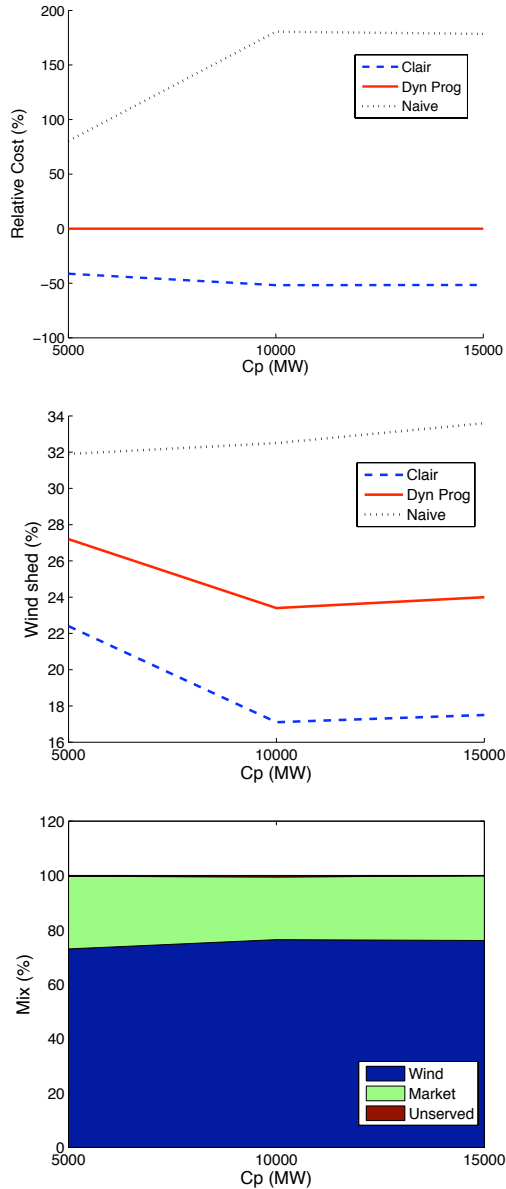


Fig. 2. Sensitivity results for varying  $C_p$ .

### 3.6 Sensitivity on cost of unserved energy ( $\rho$ )

In Fig. 5 we present the results of the sensitivity analysis on  $\rho$ . In this figure we present dollar amounts of real-time market expenses, instead of expenses relative to the dynamic programming policy. The naive policy remains insensitive to  $\rho$ , whereas the dynamic programming policy incurs greater expenses in the real-time market as  $\rho$  increases. The real-time market expenses of the clairvoyant policy are insensitive to  $\rho$ . We do not present sensitivity results on the amount of wind shedding, and the mix which is used to satisfy demand since these results are insensitive to  $\rho$ . It is noted that for the minimum price of unserved energy,  $\rho = 1,000$  \$/MWh, the clairvoyant policy deliberately leaves load unserved for some of the day types as this is more economical than buying from the market during periods of high prices, whereas for higher values of  $\rho$  the clairvoyant policy never leaves load unserved unless the other constraints in the problem force

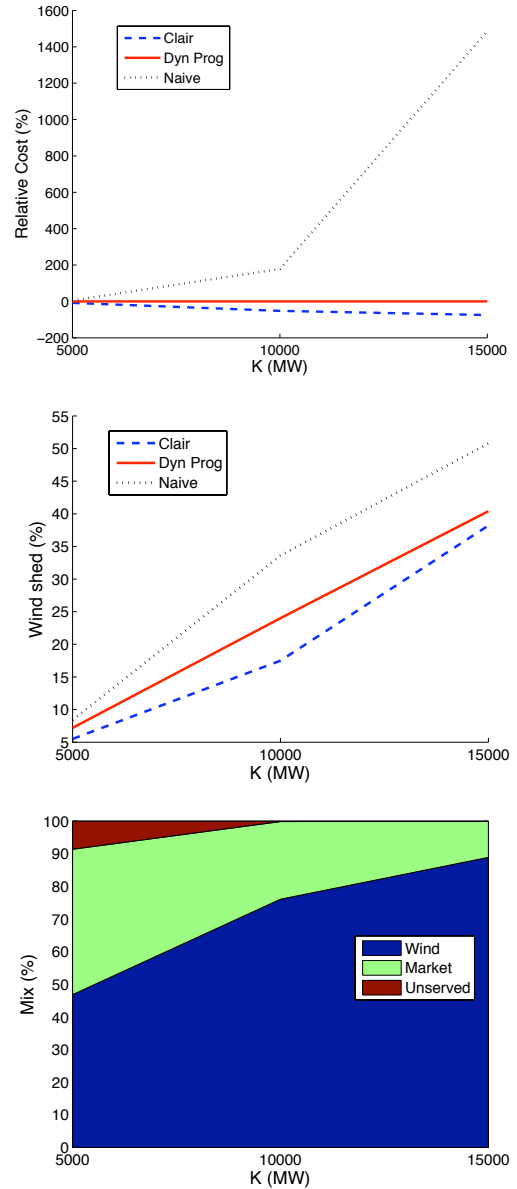


Fig. 3. Sensitivity results for varying  $K$ .

such an outcome. Moreover, for  $\rho = 1,000$  \$/MWh the dynamic programming policy has 348 MWh of unserved load, approximately three times greater than the amount of unserved load for  $\rho = 5,000$  \$/MWh, which is equal to 112 MWh.

## 4. CONCLUSION

We have proposed a contract for utilizing renewable generation to mitigate the impacts of renewable power variability and unpredictability. The contract transfers the risk of not serving load from the system operator to consumers, and results in an optimal control problem in which an aggregator seeks to optimize the extent to which loads are backed up by a volatile spot market for electricity. We compare four policies for serving flexible loads, the dynamic programming policy, the clairvoyant policy, a naive policy and a model predictive control policy. For the baseline scenario we find that the model predictive

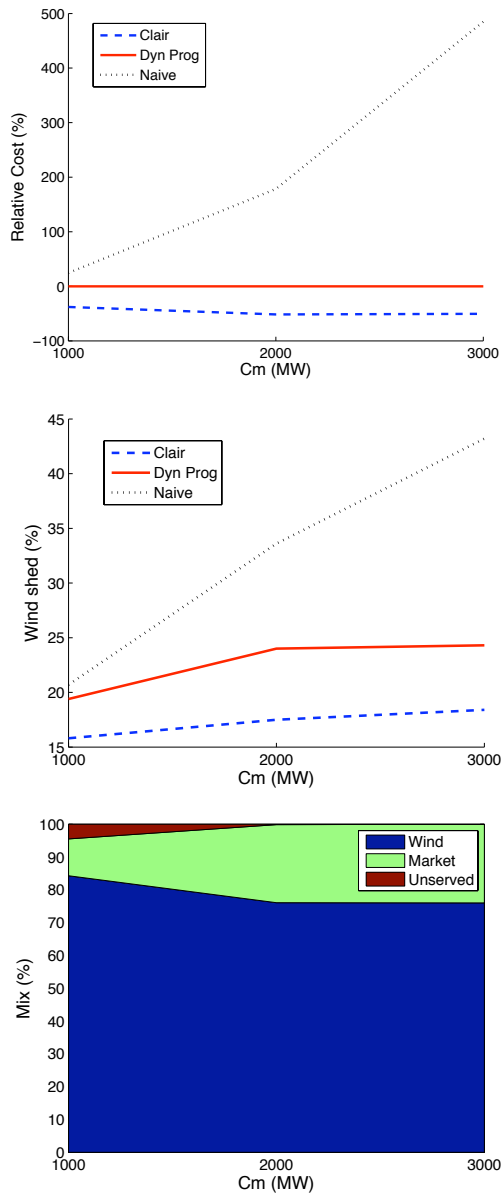


Fig. 4. Sensitivity results for varying  $C_m$ .

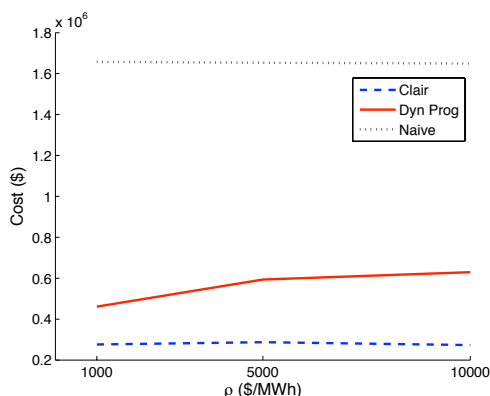


Fig. 5. Sensitivity results for varying  $\rho$ .

control policy incurs lower real-time market costs than the naive policy, however it is not able to outperform the naive charging policy overall, due to large penalties for unserved load. We also present sensitivity results on real-time market expenditures, wind power utilization, and the optimal mix for serving energy requests with respect to various problem parameters.

## REFERENCES

- Borenstein, S., Jaske, M., and Rosenfeld, A. (2002). Dynamic pricing, advanced metering and demand response in electricity markets. Technical report, University of California Energy Institute.
- CAISO (2010). The California ISO controlled grid generation queue as of January 8, 2010. URL <http://www.caiso.com/14e9/14e9ddd1ebf0.pdf>.
- Callaway, D. (2010). Sequential reliability forecasting for wind energy: Temperature dependence and probability distributions. *IEEE Transactions on Energy Conversion*, 25, 577–585.
- Deng, S.J. and Oren, S.S. (2003). Incorporating operational characteristics and start-up costs in option-based valuation of power capacity. *Probability in the Engineering and Informational Sciences*, 17, 155–181.
- Deng, S.J. and Oren, S.S. (2005). *Applications of Stochastic Programming*, chapter 31, 655–667. MPS-SIAM Series on Optimization.
- Eto, J. (2007). Demand response spinning reserve demonstration. Technical report, Lawrence Berkeley National Laboratory.
- Hirst, E. and Kirby, B. (1997). Ancillary-service details: Dynamic scheduling. Technical report, Oak Ridge National Laboratory.
- Hirst, E. and Kirby, B. (1999). Load as a resource in providing ancillary services. Technical report, Oak Ridge National Laboratory.
- Kirby, B.J. (2003). Spinning reserve from responsive loads. Technical report, Oak Ridge National Laboratory.
- Loutan, C. and Hawkins, D. (2007). Integration of renewable resources. transmission and operating issues and recommendations for integrating renewable resources on the california iso-controlled grid. Technical report, California Independent System Operator.
- Morales, J.M., Minguez, R., and Conejo, A.J. (2010). A methodology to generate statistically dependent wind speed scenarios. *Applied Energy*, 87, 843–855.
- Most, D. and Keles, D. (2009). A survey of stochastic modelling approaches for liberalised electricity markets. *European Journal of Operations Research*, 207(2), 543–556.
- Papavasiliou, A., Oren, S.S., and O’Neill, R.P. (2010). Reserve requirements for wind power integration: A scenario-based stochastic programming framework. *Accepted for publication in Transactions for Power Systems*. URL <http://www2.decf.berkeley.edu/~tonypap/publications.html>.
- Torres, J.L., Garcia, A., Blas, M.D., and Francisco, A.D. (1984). Time series models to simulate and forecast wind speed and wind power. *Journal of Climate and Applied Meteorology*, 23, 1184–1195.
- Torres, J.L., Garcia, A., Blas, M.D., and Francisco, A.D. (2005). Forecast of hourly wind speed with ARMA models in Navarre (Spain). *Solar Energy*, 79(1), 65–77.